Optical filter wavefront distortion: out-of-band to in-band predictions and the effect of the illumination source bandwidth

Graham Carlow,* [ORCID] Jean-Michel Guay, Alex Christou, Claude Montcalm, Adam Badeen, and Brian T. Sullivan

Iridian Spectral Technologies Ltd., 2700 Swansea Crescent, Ottawa, Ontario K1G6R8, Canada
Corresponding author: graham.carlow@iridian.ca

The wavefront distortion (WFD) of a surface with an optical filter coating is ideally measured at the operating wavelength (λ) and angle of incidence (θ) of the filter. However, this is not always possible, requiring that the filter be measured at an out-of-band wavelength and angle (typically $\lambda = 633$ nm and $\theta = 0°$). Since the transmitted wavefront error (TWE) and reflected wavefront error (RWE) can depend on the measurement wavelength and angle, an out-of-band measurement may not give an accurate characterization of the WFD. In this paper, we will show how to predict the wavefront error (WFE) of an optical filter at the in-band wavelength and angle from a WFE measurement at an out-of-band wavelength and different angle. This method uses (i) the theoretical phase properties of the optical coating, (ii) the measured filter thickness uniformity, and (iii) the substrate's WFE dependence versus the angle of incidence. Reasonably good agreement was achieved between the RWE measured directly at $\lambda = 1050$ nm ($\theta = 45°$) and the predicted RWE based on an RWE measurement at $\lambda = 660$ nm ($\theta = 0°$). It is also shown through a series of TWE measurements using a light emitting diode (LED) and laser light sources that, if the TWE of a narrow bandpass filter (e.g., an 11 nm bandwidth centered at $\lambda = 1050$ nm) is measured with a broadband LED source, the WFD can be dominated by the chromatic aberration of the wavefront measuring system—hence, a light source that has a bandwidth narrower than the optical filter bandwidth should be used. © 2023 Optica Publishing Group

1. INTRODUCTION

Light passing through an optical filter can induce a distortion of the wavefront, which is important for minimizing in imaging and beam-steering applications. Wavefront distortion (WFD) is typically characterized by the transmitted wavefront error (TWE) and/or the reflected wavefront error (RWE) and is commonly expressed in terms of the peak-valley (PV) or root mean square (rms) properties of the wavefront. Beam distortions can result from both the underlying substrate properties (i.e., homogeneity, thickness variations, and curvature), as well as the optical coating properties (i.e., thickness non-uniformity and the transmitted/reflected phase). The optical coating can be a significant contribution to the overall WFD as has been shown both theoretically and experimentally [1–6]. Since the phase properties of the optical coating are wavelength- and angle-dependent, determining the filter's wavefront error (WFE: TWE or RWE) of the optical filter over the "in-band" (operating) wavelength and angle ranges is important so that the filter's imaging properties are properly characterized.

Measurement and characterization of the WFE of an optical filter is typically done on a commercial interferometer at near normal incidence and with a light source operating at a wavelength of 633 nm. This does not always result in proper characterization of the WFE since (i) 633 nm may not be the in-band wavelength of the optical filter; (ii) the filter may not reflect (or transmit) at 633 nm, so a measurement is not possible due to low signal levels; and (iii) the WFE at normal incidence will, in general, be different than the WFE at the operating angle for both the substrate and the coating. Recently, wavefront measuring instruments have been introduced that permit access to a wider wavelength range, typically using broadband light emitting diode (LED) sources [7]. While this may allow for WFE measurements at the in-band wavelength, there are still many cases in which the in-band wavelength of the filter is not accessible and/or the WFE of a filter is not measured at the operating angle of incidence (AOI, θ).

To overcome the limitations of accessible wavelengths in a commercial interferometer, it has been shown that the WFE of an optical filter at its in-band wavelength can be predicted from a measurement at an out-of-band wavelength [5]. This is accomplished by performing a WFE measurement at one wavelength (e.g., 633 nm) and then using the spectral-dependent phase properties of the coating combined with the measured optical

filter wavelength uniformity to accurately predict the WFE at the desired in-band wavelength. The situation becomes more complicated when the operating angle of the filter is different than the WFE measurement angle since the angular dependence of the substrate contribution will be different compared to that of the optical coating.

In this paper, we demonstrate how the WFE of a filter, at the in-band wavelength and AOI, can be predicted by a WFE measurement at different wavelength and angle, and this prediction is verified for RWE by comparison to a measurement of the RWE at the in-band wavelength and angle. In addition, we will show that the choice of the light source in a WFD measurement is important for proper characterization of the WFE—and that using a broadband light source (e.g., LED) for WFE measurement of a narrowband filter can introduce chromatic aberration of the measurement system into the WFE of the sample. That is, if the light source bandwidth is not significantly narrower than the bandwidth of the filter under test, then the measured WFE result will not be accurate.

2. WAVEFRONT MEASUREMENT

The wavefront measurements (WFMs) described in this paper were all carried out on a multi-wavelength wavefront sensor measurement instrument (WFMI) that can measure over a ~550 nm to 1100 nm wavelength range [8]. This instrument has the option to use either LED or laser light sources.

The layout for a TWE measurement is shown in Fig. 1. For a TWE measurement, first a reference WFM is taken with a reference flat (RF) in place that reflects all the light back into the instrument [Fig. 1(a)]. The flatness of the RF is PV $< \lambda/20$ at $\lambda = 633$ nm over a 150 mm diameter. After this, a sample

is inserted between the instrument and the RF, and a sample WFM is taken [Fig. 1(b)]. The reference WFM is subtracted from the sample WFM to obtain the TWE of the sample.

For a RWE measurement, a double rotating breadboard is used to allow for separate (but concentric) rotation of the sample and the RF. The layout for an RWE measurement is shown in Fig. 2. Note that when performing an RWE measurement, a RF is used during the reference WF measurement, as in Fig. 1(a). For sample WF measurements, the same RF is also present for non-zero (oblique) angles of incidence and acts as a mirror to return the light but is not present for $\theta = 0°$. This is because at normal incidence the light is reflected directly back from the sample into the wavefront instrument. Figure 2(a) shows the setup for the normal incidence sample WF measurement (no RF used), and Fig. 2(b) shows the setup for the oblique angle sample WF measurement (RF used). Note that there is a minimum oblique AOI of around 20°—this is the result of geometric limitations in the setup, where the RF would be in front of the instrument viewport. The normal incidence RWE is obtained by subtracting the normal incidence reference WF from the sample WF. The oblique incidence RWE is obtained by first dividing the normal incidence sample WF by a factor of 2 (since the sample reflectance is measured twice in this configuration) and then subtracting the reference WF.

Note that, when using the laser sources, there were no noticeable coherence effects on the WFM.

3. WAVEFRONT DISTORTION: OPTICAL COATING CONTRIBUTION ONLY

The WFD arising from the non-uniformity of an optical coating can be explained with the help of Fig. 3, which shows a
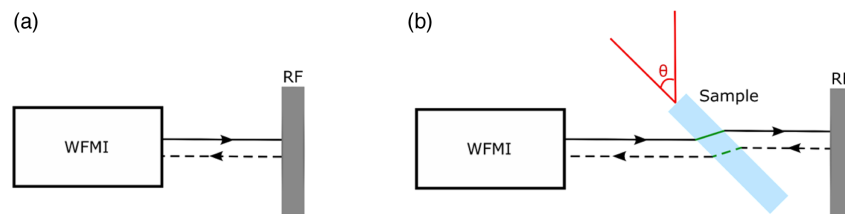
Fig. 1. Schematic for TWE measurement. (a) Reference measurement, wavefront measurement (WFM) with a reference flat (RF) only. (b) Sample measurement, the sample is inserted between the WFM instrument and the RF. In this configuration, the light is transmitted twice through the sample, which needs to be taken into account.
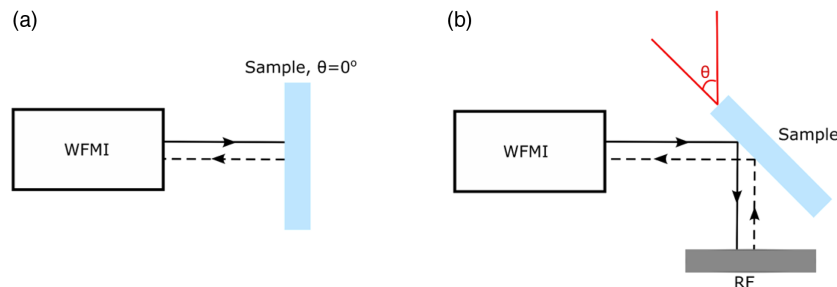
Fig. 2. Schematic for RWE measurement. (a) For the normal incidence reflectance sample measurement, the sample is inserted after the WFM instrument, but no reflectance flat is used. (b) For an oblique reflectance sample measurement ($\theta > 20°$), the sample is inserted and rotated to the desired angle of incidence, and the reflectance flat is rotated such that the light is reflected back into the WFM instrument. In this oblique angle configuration, the light is reflected twice from the sample, which needs to be taken into account. Note: the reference WFM setup required for the RWE measurement is the same as that depicted in Fig. 1(a).
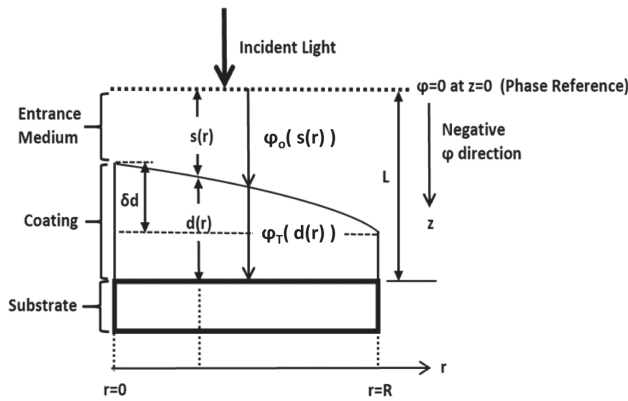
Fig. 3. Schematic of light incident upon a non-uniform optical coating (may consist of multiple layers). An arbitrary phase reference line is placed a distance L from the substrate. With the thin film phase convention, $\exp(-ikz)$, where k is the wavenumber, the phase becomes more negative along the positive z direction. In this schematic, the angle of incidence θ_o is $0°$, and the entrance medium has a refractive index n_o. The phase change across the entrance medium starting from the phase reference line is represented by φ_o while φ_T is the phase change from the coating interface to the substrate interface. At any radius, r, the distance in the entrance medium from the phase reference line to the coating interface is $s(r)$ while the coating thickness is $d(r)$. The difference in thickness at any radius r is given by $\delta d(r) = d(r = 0) - d(r)$, thus ensuring that the sign of δr is consistent with the z direction.

schematic of a light ray incident upon a non-uniform optical coating. For simplicity, this section is focused on TWE, but a similar argument can be applied to RWE. The phase convention and notations are defined in the figure caption. Note that any substrate curvature arising from coating stress is neglected in this diagram.

Using the notation of [5], the transmitted phase variation at a radius r, φ_{WF}, is the sum of the phase variation in the entrance medium and in the coating, φ_o and φ_T, respectively. If the coating thickness is d at a radius r, then since $s(r) + d(r) = L$, the phase variation resulting in a WFD can be written as

$$\varphi_{\mathrm{WF}}(\lambda, d, \theta) = \varphi_T(\lambda, d, \theta) + \varphi_o(\lambda, L - d, \theta), \quad \textbf{(1)}$$

where $\varphi_o(\lambda, z, \theta) = \dfrac{-2\pi \cdot n_o \cdot z \cdot cos(\theta_o)}{\lambda}$,

where $\varphi_T(\lambda, d, \theta)$ can be calculated from the filter design (i.e., using a thin film program) and θ is the AOI. As pointed out in [5], it is important to include the entrance medium phase contribution: for RWE the entrance medium contribution, $\varphi_0(\lambda, L - d, \theta)$, needs to be counted twice, while for TWE it is counted only once. The WFD is then given by $-\lambda \cdot \varphi_{WF}(\lambda, d, \theta)/2\pi$ [in nm], where the minus sign is required to convert from the thin film phase convention to the optics phase convention. The next step is to calculate the difference in the WFD resulting from a coating non-uniformity, i.e., between a thickness "$d + \delta d$" and "d",

$$\Delta \mathrm{WFD} = \frac{-\lambda}{2\pi} \{ \varphi_{\mathrm{WF}}(\lambda, d + \delta d, \theta) - \varphi_{\mathrm{WF}}(\lambda, d, \theta) \}, \quad \textbf{(2)}$$

where ΔWFD is in units of the wavelength, i.e., nm. Using Eq. (1),

$$\Delta \mathrm{WFD} = \frac{-\lambda}{2\pi} \{ [\varphi_T(\lambda, d + \delta d, \theta) - \varphi_T(\lambda, d, \theta)]$$
$$+ \varphi_o(\lambda, -\delta d, \theta) \}, \quad \textbf{(3)}$$

where ΔWFD is the portion of the distortion resulting from the optical coating non-uniformity and the coating's phase variation with thickness. Therefore, the WFD of a thin film coating can be calculated from the measured coating thickness uniformity and the phase properties of the coating. The change in phase with coating thickness can be directly related to the group delay, $\mathrm{GD} = -\partial\varphi/\partial\omega$, where ω is the angular frequency. The GD is, in general, a function of wavelength and angle for a thin film optical filter and is, therefore, a useful quantity to describe the wavelength- and angle-dependent phase properties of an optical coating.

It should be specifically noted that the coating WFD contribution, as described, contains part of the entrance medium WFD contribution that results from the non-uniformity of the thin film coating: this is represented by the $\varphi_o(\lambda, -\delta d, \theta)$ term in Eq. (3). Other contributions of the entrance medium, resulting from the surface figure of the substrate, are dealt with separately as discussed in the next section.

4. WAVEFRONT DISTORTION: SUBSTRATE CONTRIBUTION ONLY

The substrate contribution to the WFD will now be considered: first for TWE and then RWE. The TWE of a substrate will depend on thickness variation, refractive index homogeneity, and, to a small degree, the curvature. Assuming that the refractive index homogeneity variation is negligible, then the TWE will depend primarily on the thickness variation in the substrate. Referring to Fig. 4(a), the optical path length from point "a" to point "b" will depend on the thickness of the substrate, d, and the AOI, θ. For a given angle, the TWE will scale with any thickness variations, δd, of the substrate, and it is straightforward to show that the change in the TWE with angle is

$$\mathrm{TWE_{sub}}(\lambda, \theta) = \mathrm{TWE_{sub}}(\lambda, 0°) \cdot \frac{n_2 - n_1 \cdot \cos(\theta - \varphi)}{(n_2 - n_1) \cdot \cos(\varphi)}, \quad \textbf{(4)}$$

where n_2 and n_1 are the refractive indices of the substrate and the entrance/exit medium, respectively, and φ is the angle of refraction in the substrate. The TWE of the substrate will be independent of the wavelength if there is no significant dispersion of the refractive indices of the incident medium and the substrate.

Verification of Eq. (4) was carried out by measuring the TWE of an uncoated, 63.5 mm square, fused silica substrate, at different angles of incidence using a light source at 633 nm. Figure 4(b) shows a reasonably good agreement between the measured and predicted [based on Eq. (4)] normalized $\mathrm{TWE_{sub}}$(rms) values for various angles of incidence.

For the case of RWE substrate contribution, the $\mathrm{RWE_{sub}}$(rms) is dominated by the surface figure, i.e., surface roughness and curvature. Referring to Fig. 5(a), it can be
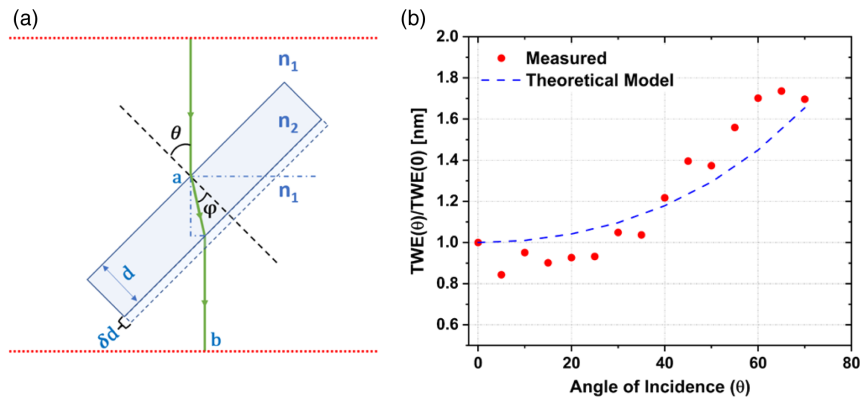
Fig. 4. (a) Schematic of a plane wave incident on a substrate at angle of incidence θ. (b) Plot of measured TWE (rms) of a substrate, normalized to TWE (at $\theta = 0°$), versus angle of incidence and the theoretical predication based on Eq. (4). The TWE (rms) at $0°$ is 15.1 nm.
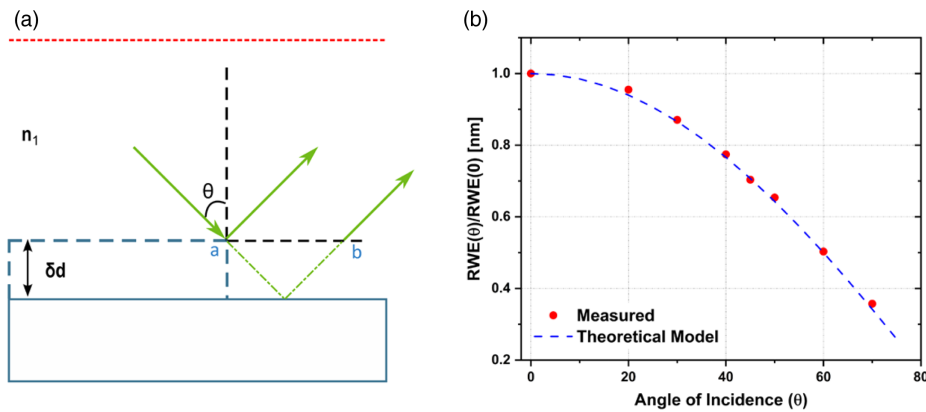
Fig. 5. (a) Schematic of a plane wave incident on a substrate at an incident angle θ. A variation in substrate thickness, δd, that gives rise to $RWE_{sub}(\lambda, 0°)$ will cause RWE_{sub} to change with the angle of incidence according to Eq. (5). (b) RWE (rms) measurement, normalized to RWE (at $\theta = 0°$), of a bare substrate, versus angle and comparison to Eq. (5). The RWE_{sub} (rms) at $\theta = 0°$ is 844 nm.

shown that, as the measurement angle (θ) is changed, the change in RWE due to thickness variations in the substrate will be as follows:

$$RWE_{sub}(\lambda, \theta) = RWE_{sub}(\lambda, 0°) \cdot \cos(\theta). \qquad (5)$$

To verify this relation, the RWE of a polished steel disk with a large curvature was measured using a LED light source at $\lambda = 625$ nm at different angles of incidence, θ. A polished steel disk was used to get a wavelength-independent reflected wavefront to simplify the demonstration. Fig. 5(b) shows a good agreement between the measured and predicted [based on Eq. (5)] normalized RWE_{sub}(rms) values for various angles of incidence.

For completeness, here is a brief discussion of how the substrate TWE is affected by a refractive index inhomogeneity (Δn_{max}) in the substrate. The substrate refractive index inhomogeneity is typically specified by a homogeneity grade (HG) such that $\Delta n_{max} = [(HG[ppm])] \times 10^{-6} \cdot n$, where n is the substrate refractive index. If we assume that light is incident upon a substrate of thickness d that is perfectly parallel but where there is a difference in index (spatially across the substrate) arising from the homogeneity, then there is a WFD (TWE_{HG} [PV]) caused by the difference in the optical path length of the minimum and maximum index regions,

$$TWE_{HG} [PV] = \Delta n_{max} \cdot d \text{ [nm]} = (HG) \times 10^{-6} \cdot n \cdot d \text{ [mm]} \times 10^6$$

$$= (HG \text{ [ppm]}) \cdot n \cdot d \text{ [mm]}.$$

For a substrate with a refractive index of $n = 1.44$ and a thickness $d = 5$ mm, changing the HG from 1 ppm to 5 ppm will increase the TWE_{HG}[rms] by a factor of 5 (from 1.5 nm rms to 7.5 nm rms). For imaging applications, it is important to use a substrate with a good homogeneity grading.

5. PREDICTION of RWE

Using the WFD properties of the thin film coating and the substrate contributions as established above, we are now in a position to describe a method for predicting the WFE of an optical filter at an operating (in-band) wavelength and angle (λ_i, θ_i) based on a WFE measurement at a different (out-of-band) wavelength and angle (λ_o, θ_o).

We will first consider the following RWE algorithm: (a) starting with an RWE measurement and a measured filter thickness uniformity, decouple the coating and substrate RWE contributions; (b) modify separately the coating and substrate RWE contributions to correct for the operating wavelength and AOI; (c) finally, recombine the modified coating and substrate RWE contributions to predict the total RWE of the optical filter at the operating wavelength and AOI.

In more detail:

1. Measure the RWE of an optical filter at an out-of-band wavelength λ_o, and AOI $\theta_o = 0°$ to get $\mathrm{RWE_{total}}(\lambda_o, 0°)$. This example uses $\theta_o = 0°$; however, an oblique angle could also be used for the out-of-band measurement.

2. Determine the variation of the optical thickness of the filter coating across the filter clear aperture—typically a center wavelength measurement for a bandpass filter. In addition, from the coating design, calculate the phase properties of the coating at both $(\lambda_o, 0°)$ and (λ_i, θ_i) [using Eq. (3)] to provide

$$\mathrm{RWE_{coating}}(\lambda_o, 0°) \text{ and } \mathrm{RWE_{coating}}(\lambda_i, \theta_i).$$

3. Decouple the substrate contribution from the out-of-band measurement as follows:

$$\mathrm{RWE_{sub}}(\lambda_o, 0°) = \mathrm{RWE_{total}}(\lambda_o, 0°) - \mathrm{RWE_{coating}}(\lambda_o, 0°).$$

4. Adjust the substrate RWE contribution to correspond to the operating AOI (θ_i) based on Eq. (5),

$$\mathrm{RWE_{sub}}(\lambda, \theta) = \mathrm{RWE_{sub}}(\lambda, 0°) \cdot \cos(\theta),$$

where, neglecting dispersion in the entrance medium, $\mathrm{RWE_{sub}}(\lambda_i, \theta_i) = \mathrm{RWE_{sub}}(\lambda_o, 0°) \cdot \cos(\theta_i)$.

5. Finally, combine the modified RWE contributions of the coating and substrate to obtain the total RWE at the operating (in-band) wavelength and angle,

$$\mathrm{RWE_{total}}(\lambda_i, \theta_i) = \mathrm{RWE_{coating}}(\lambda_i, \theta_i) + \mathrm{RWE_{sub}}(\lambda_i, \theta_i).$$

A similar procedure can be followed to obtain $\mathrm{TWE_{total}}(\lambda_i, \theta_i)$, with the only difference being that the angular dependence of the substrate TWE contribution is given by Eq. (4) instead of Eq. (5).

6. APPLICATION OF THE RWE PREDICTION ALGORITHM

To demonstrate the above RWE measurement/prediction procedure, a 23-µm-thick coating was designed and grown on a 125-mm-diameter substrate using a magnetron sputtering process. The coating had reflectance bands ($R > 99.9\%$ for s and p polarizations) at $\lambda_o = 660$ nm ($\theta_o = 0°$) and $\lambda_i = 1050$ nm

($\theta_i = 45°$) with corresponding GDs of 0.065 ps and 0.31 ps, respectively [Fig. 6(a)]. The difference in GD was intentional in the design so as to create a difference in RWE of the coating in the two reflectance bands. Since a perfectly uniform coating would not give rise to any coating RWE contribution, an intentional thickness non-uniformity of ∼0.3%, over a 40 mm radius, was introduced for this demonstration filter [Fig. 6(b)].

The RWE WFMs were carried out using laser sources at $\lambda_o = 660$ nm and $\lambda_i = 1050$ nm. The measured and predicted RWE profiles across a 78-mm-diameter clear aperture of the substrate are shown in Fig. 7. Figure 7(a) shows the measured RWE of the filter at $\lambda_o = 660$ nm ($\theta_o = 0°$) along with the decoupled substrate and coating contributions. As can be seen, the coating contribution is quite small since the GD at $\lambda_o = 660$ nm is relatively small for this filter. The relatively large substrate RWE contribution arises from the curvature of the substrate caused by coating stress. Using the angular dependence of the substrate RWE, and the coating phase properties based on the coating design and the measured coating uniformity, the individual substrate and coating contributions at $\lambda_i = 1050$ nm ($\theta_i = 45°$) were determined as shown in Fig. 7(b). Note that the RWE coating contribution has changed significantly with the difference in wavelength and AOI. In particular, the direction of the RWE has gone from "concave down" [Fig. 7(a)] to "concave up" [Fig. 7(b)]. This comes about because of the detailed phase properties of the coating at the two wavelengths and angles and also because of the change in the entrance medium contribution that results from the coating non-uniformity [Eq. (3)]. Finally, after recombining the modified substrate and coating contributions, Fig. 7(c) shows the predicted total RWE at $\lambda_i = 1050$ nm ($\theta_i = 45°$), along with a direct measurement of the RWE measurement at $\lambda_i = 1050$ nm ($\theta_i = 45°$). Note in this specific case that the coating and substrate contributions in Fig. 7(b) are curved in opposite directions, so when added, the resultant RWE is reduced. As can be seen, the measurement and prediction values are in good agreement. In addition, Fig. 7(c) also shows the RWE measurement at $\lambda_o = 660$ nm ($\theta_o = 0°$) as a comparison to the actual RWE measurement indicating the out-of-band RWE measurements are, in general, not an accurate representation of the RWE at the in-band (operating) wavelength and AOI.
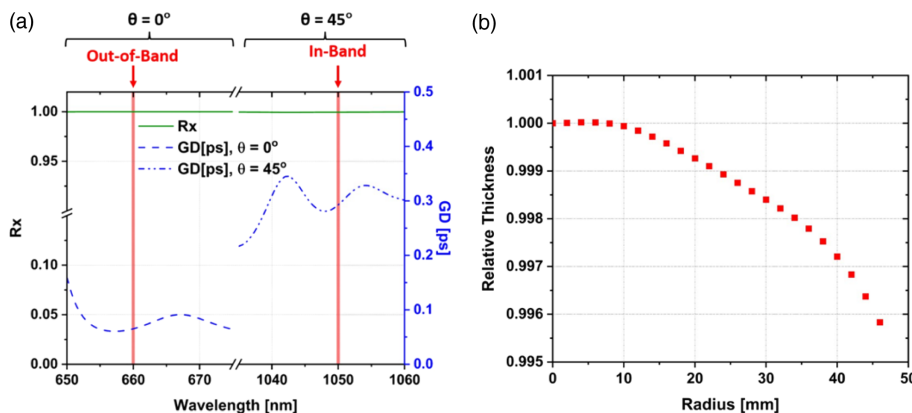
Fig. 6. RWE demonstration filter. (a) Reflectance and GD at $\lambda_o = 660$ nm ($\theta_o = 0°$) and $\lambda_i = 1050$ nm ($\theta_i = 45°$). (b) Measured thickness uniformity variation over a radius of 45 mm. The thickness is normalized to unity at the center of the substrate (radius = 0 mm).
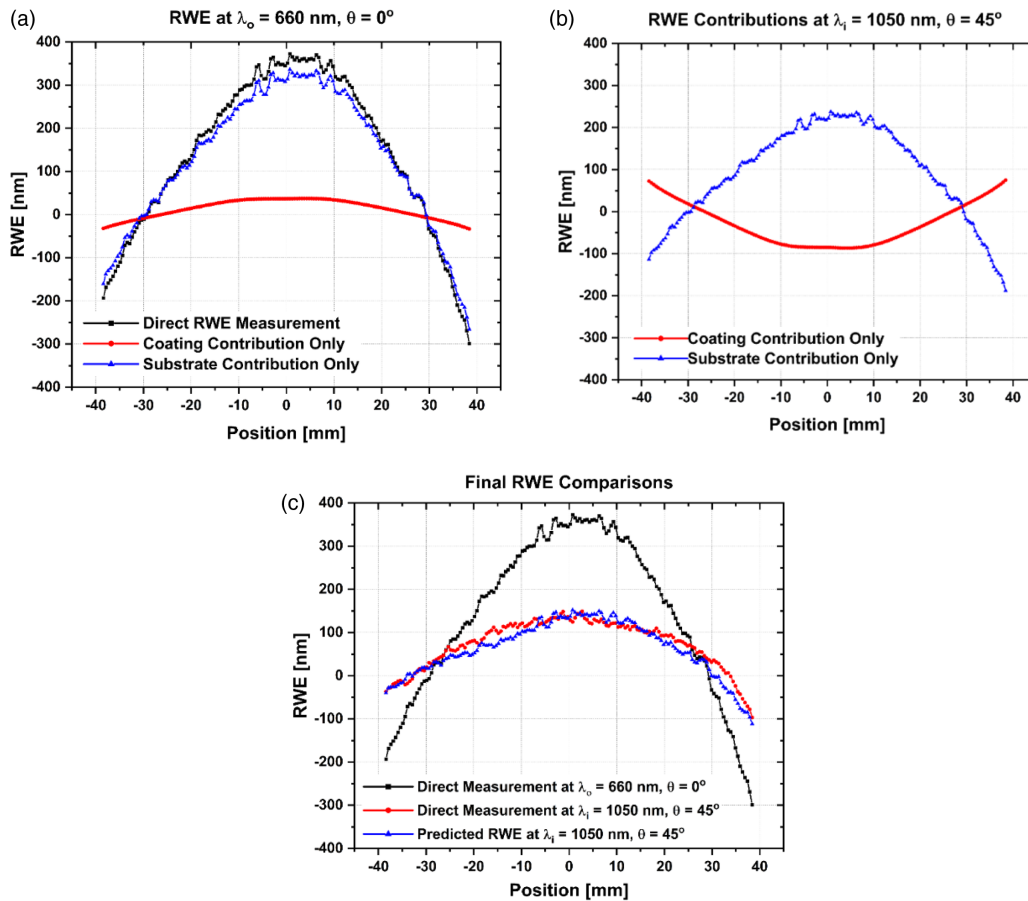
Fig. 7. RWE measurements and calculations. (a) RWE at out-of-band wavelengths/AOI. (b) RWE of substrate and coating at in-band wavelength/AOI. (c) RWE measured and calculated at the in-band wavelength/AOI, and RWE and out-of-band wavelength/AOI.

Table 1. RWE (rms) Values, Measured and Calculated, at the Different Wavelengths and Angles, for the RWE Demonstration Filter

	Measurement 660 nm, 0°	Substrate 660 nm, 0°	Coating 660 nm, 0°	Substrate 1050 nm, 45°	Coating 1050 nm, 45°	Predicted RWE 1050 nm, 45°	Measured RWE 1050 nm, 45°
RWE Contribution (rms)	180.6 nm	158.9 nm	21.9 nm	112.4 nm	50.1 nm	62.8 nm	56.4 nm

To better compare the different RWE values, Table 1 shows the RWE (in nm rms) for all measured and calculated RWE contributions; the RWE prediction at $\lambda_i = 1050$ nm ($\theta_i = 45°$) is within about 10% of the measured RWE value. Note that some of the difference between the measured and calculated RWE at $\lambda_i = 1050$ nm ($\theta_i = 45°$) can be a result of the RF being in the beam path for the sample measurement at $\theta_i = 45°$, but not in the beam path for the sample measurement at $\theta_o = 0°$ (i.e., the RF is not perfectly flat).

7. IMPORTANCE OF LIGHT SOURCES IN WFE MEASUREMENTS

As mentioned previously, a typical WFD measurement of an optical filter first involves the WFM of a RF without the optical filter (reference wavefront) followed by a sample measurement with the filter in place (sample wavefront). Then the reference wavefront is subtracted from the sample wavefront to remove

aberrations of the wavefront measuring system and, hence, get the true sample wavefront. However, for applications where the optical filter is a narrow bandpass filter, it is important to use a narrowband illumination source (i.e., where the source bandwidth is less than the bandwidth of the filter) for the WFD measurements. The reason is that wavefront sensors, using lenses to produce a collimated beam, have a wavelength-dependent focal length (i.e., chromatic aberration), so when taking a reference measurement with a broadband light source, there will be many wavelengths out of focus that contribute to the WFD of the reference measurement. However, when taking a sample WFM where the sample is a narrow bandpass filter, only a limited range of wavelengths is transmitted through the filter, and some of the chromatic aberrations that are present in the reference measurement are filtered out in the sample measurement. The net result is that, if the illumination bandwidth is wider than the filter bandwidth, the WFE measurement will

Table 2.   TWE Measurement Setups at $\lambda = 1050$ nm Using a Different Combination of Light Sources and Filters

Measurement	Light Source Used for Reference Measurement	Light Source Used for Sample Measurement	Type of Filter Used in Measurement
M1	LED	LED	11 nm NBF
M2	LED	Laser	none
M3	Laser	Laser	11 nm NBF

have a component that depends on the chromatic aberration of the optical system, which is not representative of the sample being measured.

To demonstrate this for TWE, a series of three TWE measurements was taken at normal incidence using different combinations of light sources as outlined in Table 2. The sample used in these measurements was an 80-mm-diameter, 11 nm narrow bandwidth filter (NBF), centered near $\lambda \sim 1050$ nm ($\theta = 0°$). The LED source was a Thorlabs M1050F3, which has a FWHM of $\sim$50 nm and whose spectral intensity is shown in Fig. 8(a) along with the transmittance of the 11 nm NBF (sample).

The idea behind these different measurement setups is the following:

• M1 results in a TWE that is a combination of the chromatic aberration of the system (from the reference measurement) and the TWE of the filter (from the sample measurement).
• M2 measures the chromatic aberration of the system only. This is because, with no physical sample in place during the "sample measurement" with the laser, the TWE will reveal the chromatic aberration that is present during the LED reference measurement.
• M3, using the laser for both the reference and sample measurements, measures more accurately the TWE of the sample (with no contribution from the chromatic aberration of the system).

Note that a reasonable approximation from these three measurements is $\text{TWE}_{M3} \approx \text{TWE}_{M1} - \text{TWE}_{M2}$.

Shown in Fig. 8(b) is the TWE (with piston and tilt removed) across the diameter of the sample for the measurement setups M1, M2, and M3. For measurement M2, the PV difference is 560 nm, which is large considering that, for an ideal system with no chromatic aberration, the PV should be $\sim$0 nm.

The TWE_{rms} values for M3 and (M1-M2) are 41.7 nm and 40.5 nm, respectively, which show a very good agreement. Note that the WFD of a filter is sensitive to the specific wavelength being sampled within the filter bandpass region. Hence, some of the difference between $(\text{TWE}_{M1} - \text{TWE}_{M2})$ and TWE_{M3} can arise as the LED source used in the M1 sample measurement will illuminate the entire bandpass of the filter rather than just the monochromatic wavelength of the laser.

Therefore, LED illumination used in the instrument when measuring the TWE of the 11 nm filter (M1) results in the TWE measurement being dominated by the chromatic aberration of the measurement system (which is quite large in this case). This example clearly shows the need for a narrowband illumination source. To reduce any artefacts of the TWE measurement that result from chromatic aberration of the measurement system, the filter under test should pass all wavelengths of the illumination source over its entire clear aperture. This essentially means that the illumination spectrum should be entirely contained within the filter bandpass, accounting for the wavelength variation of the filter, and can be accomplished by either using a laser source or by using an LED source in combination with a sufficiently narrow bandpass filter.

8. SUMMARY

In this paper, it has been shown that the WFD of optical filter can be predicted at a wavelength and AOI based on (i) a WFE measurement at a different wavelength and/or AOI; (ii) the thickness uniformity of the optical filter; and (iii) the phase properties of the optical coating at the different wavelength and angles. For RWE, the predictions were confirmed by a direct measurement of an RWE demonstration filter. This method is useful for determining the WFD of a filter when a WFM system is not set up for measurements at desired wavelengths and/or angles of incidence.
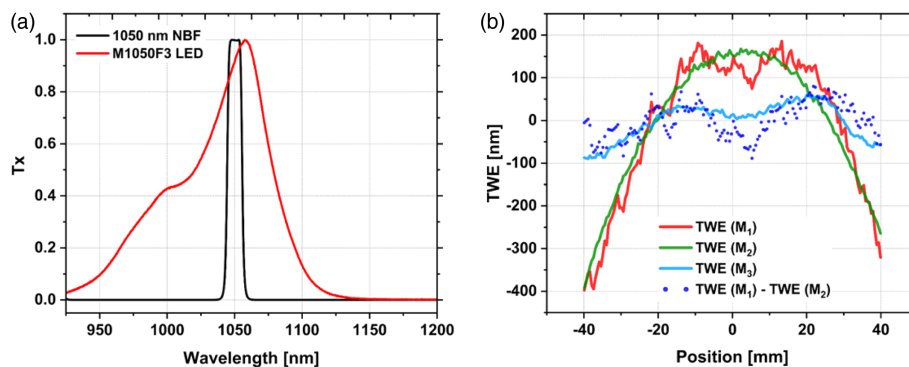
Fig. 8.   (a) Normalized LED Spectrum and the transmittance of the NBF. (b) TWE line scan across diameter of the sample showing TWE_{M1}, TWE_{M2}, TWE_{M3}, and $\text{TWE}_{(M1)} - \text{TWE}_{(M2)}$.

It has also been demonstrated that WFE measurements of spectrally narrow bandpass filters should be done with an illumination source that is spectrally narrower than the filter's bandwidth. If this is not done, then chromatic aberration of the measurement system will be present in the WFE measurement resulting in significant systematic errors.

Disclosures.   The authors declare no conflicts of interest.

Data availability.   Data underlying the results presented in this paper are not publicly available at this time but may be obtained from the authors upon reasonable request.

REFERENCES

1. P. Baumeister, *Optical Coating Technology* (SPIE, 2004).
2. A. McLeod, *Phase Matters* (SPIE Newsroom, 2005).
3. M. Vergöhl, C. Britze, S. Bruns, A. Pflug, J. Zimara, B. Schäfer, K. Mann, and V. Kirschner, "Uniformity and wavefront control of optical filters," Proc. SPIE **11180**, 1118046 (2019).
4. A. Piegari and A. Sytchkova, "Phase distortion and thickness variation in the design of optical coatings," Proc. SPIE **10562**, 105621H (2016).
5. G. Carlow, B. T. Sullivan, C. Montcalm, and A. Miles, "Effect of an optical coating on in-band and out-of-band transmitted and reflected wavefront error measurements," Appl. Opt. **59**, A135–A142 (2020).
6. L. M. G. Venancio, L. Carminati, J. L. Alvarez, J. Amiaux, L. Bonino, J.-C. Salvignol, R. Vavrek, R. Laureijs, A. Short, T. Boenke, and P. Strada, "Coating induced phase shift and impact on Euclid imaging performance," Proc. SPIE **9904**, 99040V (2016).
7. W. Boucher, B. Wattellier, and V. D. Genuer, "Multi-wavelength large optics wavefront error metrology bench," Proc. SPIE **11116**, 111160V (2019).
8. Phasics, Filters and Polarizing Optics Testing | Phasics – Phasics, https://www.phasics.com/en/application-areas/optics-systems-metrology/filters-and-polarizing-optics-metrology/.